

A Determination of the Structure of the Intramolecular Charge Transfer State of 4-Dimethylaminobenzonitrile (DMABN) by Time-Resolved Resonance Raman Spectroscopy

W. M. Kwok,^{*,†} C. Ma,[†] P. Matousek,[‡] A. W. Parker,[‡] D. Phillips,[†] W. T. Toner,[§] M. Towrie,[‡] and S. Umaphy[⊥]

Department of Chemistry, Imperial College of Science, Technology and Medicine, Exhibition Road, London SW7 2AY, U.K.; Central Laser Facility, CLRC Rutherford Appleton Laboratory, Didcot, Oxfordshire OX11 0QX, U.K.; Department of Physics, Clarendon Laboratory, Parks Road, Oxford OX1 3PU, U.K.; and Department of Inorganic and Physical Chemistry, Indian Institute of Science, Bangalore, India

Received: October 9, 2000; In Final Form: November 28, 2000

Picosecond time-resolved resonance Raman spectra of the A (intramolecular charge transfer, ICT) state of DMABN, DMABN-*d*₆ and DMABN-¹⁵N have been obtained. The isotopic shifts identify the $\nu^s(\text{ph-N})$ mode as a band at 1281 cm⁻¹. The ~ 96 cm⁻¹ downshift of this mode from its ground state frequency rules out the electronic coupling PICT model and unequivocally supports the electronic decoupling TICT model. However, our results suggest some pyramidal character of the A state amino conformation.

Introduction

4-Dimethylaminobenzonitrile (DMABN) is an archetypal electronic donor–acceptor molecule that undergoes intramolecular charge transfer (ICT) accompanied by structural reorganization in the solution phase.¹ Since its discovery in 1951, the solvent-dependent dual fluorescence phenomenon of DMABN has been rationalized in terms of a nonradiative conversion between a local excited (LE) and an ICT state, termed B and A states, respectively. The forward ICT reaction dominates in polar solvents. Monomolecular models interpreting the nature and structure of the A state fall into four main classes: TICT (twisted intramolecular charge transfer),² WICT (wagged ICT),³ PICT (planar ICT),⁴ and RICT (rehybridization ICT).⁵ All have an ICT mechanism in common but they differ in modes related to the B to A conversion.

Many experimental and theoretical studies have been devoted to investigating and evaluating the proposed models. From the theoretical point of view, the A state structures suggested by the TICT,^{6–8} PICT,⁷ and RICT⁵ models are all found to exist as local minima on the S₁ potential energy surface. However, the RICT model was ruled out because of a large activation barrier for the B to A transition.^{8,9} The validity of the WICT model is also doubted since calculations show that a simple wagging motion of the dimethylamino group cannot, by itself, lead to the required highly polar A state (17 D).^{6,8} This leaves a combination of twisting and wagging motion of the amino group as possibilities. With the aim of discriminating between the TICT and PICT models, Dryer and Kummrow⁷ have performed full optimization ab initio CASSCF calculations. They conclude that an experimental determination of the frequency of phenyl–amino stretching mode, $\nu^s(\text{ph-N})$, will allow a final decision between the two models to be made. The

TICT model predicts a downshift of the $\nu^s(\text{ph-N})$ frequency relative to the ground state while the PICT model requires an upshift.

Direct experimental evidence for the structures of the excited states of DMABN in solution has recently been obtained using time-resolved infrared (TRIR)^{10–12} and picosecond Kerr gated time-resolved resonance Raman (ps-K-TR3) spectroscopy.^{13,14} The observation of the A state C≡N stretching mode at ~ 2100 cm⁻¹ rules out the RICT model as this model predicts a ~ 1650 cm⁻¹ C≡N frequency which is far away from that observed by both TRIR and ps-K-TR3. This leaves the remaining three models in dispute. The crucial $\nu^s(\text{ph-N})$ mode has to date not been observed using femtosecond mid-infrared spectra of DMABN in acetonitrile.¹¹ However, Okamoto¹² has recorded three bands for DMABN in acetonitrile at 960, 1216, and 1273 cm⁻¹ using picosecond infrared spectroscopy and one of these is believed to be assignable to the $\nu^s(\text{ph-N})$ vibration. In our ps-K-TR3 experiments, obtained with 267 nm pump and 330 nm probe, we have observed the C≡N stretching band, three phenyl ring modes, and bands sensitive to the dimethylamino group as shown by comparing the A state Raman spectra of DMABN and methyl-deuterated (DMABN-*d*₆).¹⁴ However, differences in the number of the bands and spectral pattern prevented direct assignment, although the absence of a strong band in the C=N double bond stretching region^{14,12} casts doubt on the PICT model. Thus identification of the $\nu^s(\text{ph-N})$ mode and assignment of the observed bands are needed to discriminate conclusively between the TICT and PICT models and elucidate the A state structure and underlying ICT mechanism.

Normal-mode analysis of ground state DMABN indicates that vibrational coupling is extensive in this molecule.¹⁵ For example, the $\nu^s(\text{ph-N})$ mode may contribute to as many as six modes and mix strongly with the vibrations from the phenyl ring.¹⁵ This presents difficulties in recognizing band shifts due to isotopic substitution and may be responsible for the significant difference of the A state ps-K-TR3 spectra between DMABN and DMABN-*d*₆.¹⁴ In spite of this complexity, it is expected that dimethylamino group ¹⁵N isotopic substitution would

* Author to whom correspondence should be addressed. E-mail: w.m.kwok@ic.ac.uk.

[†] Imperial College of Science, Technology and Medicine.

[‡] Rutherford Appleton Laboratory.

[§] Clarendon Laboratory.

[⊥] Indian Institute of Science.

selectively affect the $\nu^s(\text{ph-N})$ and $\nu(\text{NC}_2)$ stretching modes.¹⁶ In order to identify the $\nu^s(\text{ph-N})$ mode and complement our previous study on DMABN and DMABN- d_6 , we have synthesized the amino-nitrogen isotopic substituted compound, DMABN- ^{15}N and measured ps-K-TR³ spectra using a probe wavelength of 330 nm. The experiment revealed several bands sensitive to ^{15}N substitution. Similar spectra with improved spectral resolution were obtained by carrying out single-color transient resonance Raman (TR²) experiment at 330 nm excitation. As noted earlier, normal-mode analyses give conflicting results^{15,17} and this leaves the assignment of several ground state Raman bands, especially the important modes related to amino group vibration, unclear. To help clarify this situation, ground state resonance Raman spectra of the three isotopically substituted compounds were obtained using 330 nm nanosecond pulsed lasers, as well as normal Raman spectra at 532 nm probe wavelength. These results are discussed in relation to geometric and electronic structural differences between the A and ground state.

Experimental Section

The ps-K-TR³ experiments were carried out using a TR³ system based on optical parametric amplifiers (OPAs), described elsewhere.^{18,19} The pump and probe wavelengths were 267 and 330 nm with 5–10 and 1–5 $\mu\text{J}/\text{pulse}$, respectively, ~ 1 ps pulse length, and parallel polarizations. The beams were focused to 100–200 μm diameter at the sample flowing in a 500 μm diameter jet. Details of acquisition methods and the Kerr gate are given in ref 20. Here we used an improved system based on a benzene Kerr gate with throughput up to 30–40% (excluding polarizer losses) which will be reported elsewhere. A solution filter of *trans*-stilbene was used to block the Rayleigh line and scattered pump light. The filter attenuated all bands below 900 cm^{-1} . Each spectrum shown is the sum of three individual background-subtracted spectra with accumulation times typically of 2000 s.

Since both the ground and A state of DMABN absorb in the 330 nm region, ground state resonance Raman spectra and TR² spectra of DMABN, DMABN- d_6 , and DMABN- ^{15}N were obtained by the single-color pump–probe method. The TR² spectra presented were resulted from subtraction of normalized low laser power (~ 0.1 mJ/pulse) spectra and solvent spectra from high power (~ 0.5 mJ/pulse) spectra; while the ground state resonance Raman spectra were from subtraction of normalized high laser power spectra and solvent spectra from low power spectra. The 330 nm laser, ~ 20 ns pulse duration, was generated by frequency doubling of 660 nm dye (DCM) laser pulse pumped by 308 nm excimer laser. The laser beam was loosely focused (~ 0.5 mm beam diameter) onto a flowing liquid jet of sample and resonance Raman scattering was collected using backscattering geometry. The Raman scattering was imaged onto a spectrograph and collected by a liquid nitrogen cooled CCD detector. The total accumulation times for the high and low power spectra were about 1 and 2 h, respectively.

Acetonitrile Raman bands were used to calibrate the spectra with an estimated accuracy of ± 10 and ± 3 cm^{-1} in absolute frequency for ps-K-TR³ and TR² spectra, respectively. The spectra are not corrected for variations in throughput and detector efficiency.

Spectroscopic grade solvents were used as received. Commercially available DMABN was recrystallized three times before use. DMABN- d_6 and DMABN- ^{15}N were synthesized according to refs 3, 21, and 22, and the purity was confirmed by NMR and mass spectroscopic analysis. Sample concentra-

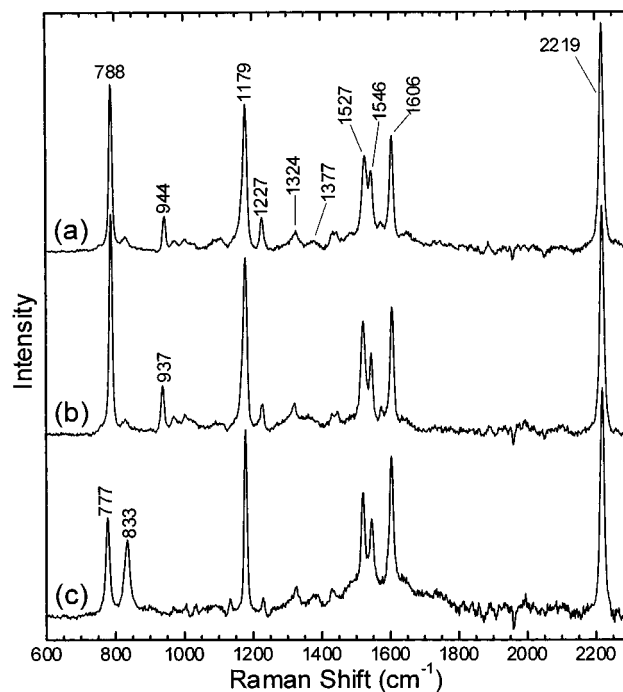


Figure 1. Resonance Raman spectra of ground state of DMABN (a), DMABN- ^{15}N (b), and DMABN- d_6 (c) obtained by 330 nm excitation in methanol solvent.

tions were $(5-10) \times 10^{-3}$ mol dm^{-3} for the ps-K-TR³ and the single-color pump–probe TR² experiments. The samples were renewed every 2 h, although UV absorption spectroscopy revealed no degradation.

Results and Spectroscopic Assignments

I. Ground-State Raman Spectroscopy. Figure 1 shows ground state resonance Raman spectra of DMABN (a), DMABN- ^{15}N (b), and DMABN- d_6 (c) in methanol solvent recorded at 330 nm excitation. Nonresonant Raman spectra of the three compounds in the solid phase obtained using 532 nm excitation are illustrated in Figure 2. Table 1 lists the Raman bands observed and their assignments. Mode analyses of ground state DMABN by Gate et al.¹⁵ and Schneider et al.¹⁷ form the main basis of our assignments. Where we differ, comparison is made with the isotopically substituted DMABN spectra and closely related compounds, such as aniline,²³ dimethylaniline (DMA), and their various isotopic substituted compounds.^{24,25} Wavenumber values of the Raman bands of DMA and DMA- d_6 are listed in Table 1.

Most of our assignments are in agreement with earlier work, especially for modes dominated by local vibrations. These are the 2219 cm^{-1} band from cyano-group $\text{C}\equiv\text{N}$ stretching vibration; intense bands at 1606, 1546, 1527, 1227, 1179, and 788 cm^{-1} which are mainly from phenyl ring vibrations described sequentially by Wilson notation 8a, 8b, 19a, 7a, 9a, and 1; and the pure methyl group C-H deformation vibration (δ_{Me}^s) at 1446 cm^{-1} manifested by its characteristic frequency and a ~ 314 cm^{-1} isotopic shift caused by deuteration of the two methyl groups^{24,25} (see the 1446 and 1132 cm^{-1} bands in DMABN and DMABN- d_6 in Figure 2, a and c, respectively).

The 1370 cm^{-1} band, seen more clearly in Figure 2, is ascribed to $\nu^s(\text{ph-N})$ based on the ~ 14 cm^{-1} downshift in DMABN- ^{15}N (1356 cm^{-1}). Schneider et al.¹⁷ attribute this band to another methyl deformation, but our assignment is consistent with the suggestion of Gate et al.¹⁵ and theoretical results from Dreyer and Kummrow.⁷ From normal coordinate analysis of

TABLE 1: Frequencies and Proposed Assignments of Raman Bands Observed for Ground State of DMABN and Its Isotopic Substituted Compounds^a

tentative assignment	ground state of DMABN			DMA ^b	
	DMABN ^c	DMABN- ¹⁵ N ^c	DMABN- <i>d</i> ₆ ^c	DMA	DMA- <i>d</i> ₆
C≡N stretching	2219(1.00)	2219(1.00)	2219(1.00)		
ring C=C stretching (8a)	1606(0.47)	1606(0.49)	1603(0.57)	1605	1600
ring C=C stretching (8b)	1546(0.37)	1545(0.23)	1546(0.29)		
ring C=C + C-C (19a)	1527(0.44)	1522(0.56)	1520(0.40)	1508	1500
δ_{Me}^s	1446 ^d	1446 ^d	1132 ^d	1450	1136
$\nu^s(\text{ph-N})$ (13)	1377/1370 ^d	1364/1356 ^d	1377/1375 ^d	1348	1343
ring in-plane C=C(14)	1324(0.11)	1318(0.22)	1322(0.15)	1335	1320
$\nu^s(\text{ph-CN})$ (7a)	1227(0.07)	1227(0.06)	1227(0.02)		
ring C-H in-plane bending (9a)	1179(0.65)	1178(0.76)	1178(0.55)	1195	1193
ρ_{Me}^s	1166 ^d	1166 ^d	1033 ^d	1160	1022
ring C-H in-plane bending (18a)	1003 ^d	1002 ^d	1003 ^d		
$\nu^s(\text{NC}_2)$	944(0.10)	937(0.14)	833(0.41)	949	828
ring breathing (1)	788(0.55)	788(0.73)	777(0.36)	744	715

^a Relative intensities of bands are indicated inside parentheses. ^b From ref 25. ^c Resulted from Lorentzian fitting of the spectra shown in Figure 1. ^d Bands are from normal Raman spectra shown in Figure 2 because of weak intensity or absence in the resonance Raman spectra (Figure 1).

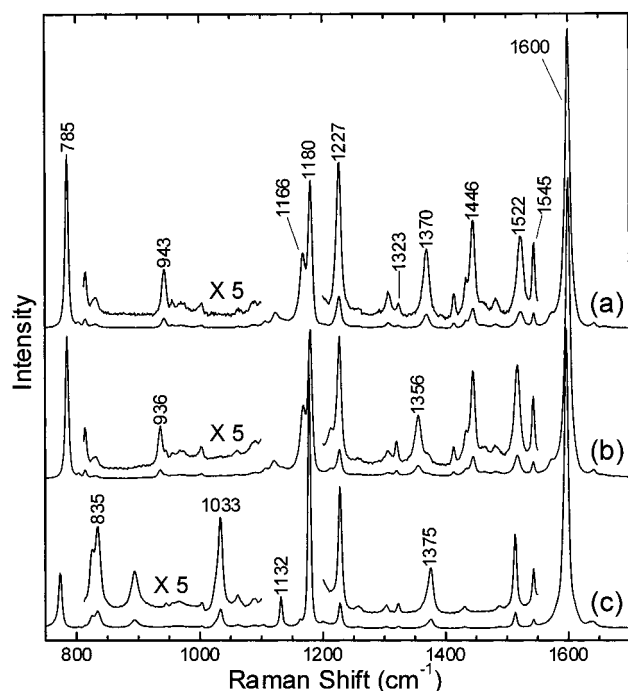


Figure 2. Nonresonance Raman spectra of solid-phase DMABN (a), DMABN-¹⁵N (b), and DMABN-*d*₆ (c) obtained by 532 nm excitation.

the closely related compound *p*-dimethylaminobenzaldehyde (DMABA), Kushto et al.²⁶ assign the 1372 cm⁻¹ band to this mode, which they describe as the Wilson 13 ring-substituent stretching mode.²⁷ This mode is found at a similar frequency in other aromatic amino compounds.^{24,25}

The mid-intensity shoulder at 1166 cm⁻¹ shown in Figure 2a,b is insensitive to ¹⁵N substitution but strongly sensitive to methyl group deuteration (Figure 2c). Although previous calculations predicted the methyl group rocking mode (ρ_{Me}^s) of DMABN at around this frequency,¹⁵⁻¹⁷ there is band congestion in this region and some workers have assigned it to various other vibrations.^{15,17} Infrared (IR) and Raman studies of dimethylamino-substituted compounds indicate that the N(CH₃)₂ substituent leads to characteristic methyl symmetric rocking vibrations at 1160 and 1025 cm⁻¹ for normal DMABN and the methyl-deuterated derivative, respectively.^{16,24-26} We therefore attribute the 1166 (DMABN and DMABN-¹⁵N) and 1033 cm⁻¹ (DMABN-*d*₆ in Figure 2c) bands to ρ_{Me}^s .

The Raman band observed at 944 cm⁻¹ shows weak sensitivity to ¹⁵N substitution (~ 7 cm⁻¹ downshift to 937 cm⁻¹ in DMABN-¹⁵N), but strong sensitivity to deuteration of the methyl groups (833 cm⁻¹). The band is therefore attributed to $\nu^s(\text{NC}_2)$ symmetric stretching vibration following Gate et al.¹⁵ rather than the ring skeleton out-of-plane Wilson 5 vibration suggested by Schneider et al.¹⁷ However, in IR measurements of various isotopic substituents of DMABN, we have found a weaker 950 cm⁻¹ band appearing as a shoulder of the 944 cm⁻¹ band, and its isotopic shift indicates that it is a ring mode. We therefore assign this band to Wilson 5. In DMA and other related compounds, such as *N,N,N',N'*-tetramethyl-*p*-phenylenediamine (TMPD) and *N,N,N',N'*-tetramethylbenzidine, the $\nu^s(\text{NC}_2)$ frequency was observed to downshift by ~ 120 cm⁻¹ upon deuteration of the methyl groups (from 949 to 828 cm⁻¹ in DMA).²⁵ This large isotopic shift has previously been verified by quantum chemical calculations and interpreted in terms of coupling between $\nu^s(\text{NC}_2)$ and methyl rocking vibrations.¹⁶ The 833 cm⁻¹ band in DMABN-*d*₆ spectra (Figures 1c and 2c) is thus ascribed as a counterpart of the 944/937 cm⁻¹ band in DMABN/DMABN-¹⁵N.

It should be mentioned that the ~ 14 and ~ 7 cm⁻¹ isotopic shift of the $\nu^s(\text{ph-N})$ and $\nu^s(\text{NC}_2)$ modes, respectively, upon ¹⁵N substitution is comparable to the 17 and 6 cm⁻¹ downshifts predicted by Brouwer et al.¹⁶ in their theoretical study of DMA. Isotopic shifts of the three amino group related modes, $\nu^s(\text{ph-N})$, $\nu^s(\text{NC}_2)$, and ρ_{Me}^s , upon deuteration of the methyl groups are also consistent with theoretical results.¹⁶

The 1324 cm⁻¹ Raman band, which is resonance enhanced at the 330 nm excitation wavelength (Figure 1), is obviously a phenyl ring mode, because it is insensitive to methyl group deuteration and only slightly sensitive to ¹⁵N substitution (Table 1). It is assigned to Wilson 14, one of the two possible modes suggested by Gate et al.¹⁵ and Schneider et al.¹⁷ This is a ring asymmetric in-plane skeletal vibration. The other possible assignment, ring C-H in-plane bending (Wilson 3), can be ruled out because the band does not show the expected significant sensitivity to ring deuteration.

II. A State DMABN Resonance Raman Spectroscopy. Ps-K-TR³ spectra of the A state of DMABN, DMABN-¹⁵N and DMABN-*d*₆ recorded in methanol solvent at 50 ps delay time are displayed in Figure 3. The probe wavelength of 330 nm falls within the strong transition from the A state of DMABN identified by Okada et al.²⁸ Figure 4 shows TR² spectra of the three compounds obtained using the 330 nm single-color

TABLE 2: Frequencies and Proposed Assignments of Raman Bands Observed for the A State of DMABN and Its Isotopic Substituted Compounds^a

tentative assignment	A state of DMABN			DMA-H ⁺ ^b	
	DMABN	DMABN- ¹⁵ N	DMABN- <i>d</i> ₆	DMA-H ⁺	DMA- <i>d</i> ₆ -H ⁺
C≡N stretching	2095(1.00)	2095(1.00)	2095(1.00)		
ring C=C stretching (8a)	1580(1.19)	1578(1.50)	1581(1.15)		
	1502(0.60)	1504(0.36)			
	1358(0.12)		1352(0.11)		
$\nu^s(\text{ph-N})$ (13)	1281(0.08)	1261(0.09)	1249(0.28)	1245	1205
$\nu^s(\text{ph-CN})$ (7a)	1221(0.06)	1221(0.04)	1212(0.21)		
ring C-H in-plane bending (9a)	1170(0.18)	1170(0.25)	1166(0.41)	1184	1187
ρ_{Me}^s	1116(0.44)	1115(0.51)	1017(0.33)	1132	1028
ring C-H in-plane bending (18a)	984(0.06)	987(0.07)	985(0.05)		
$\nu^s(\text{NC}_2)$	907(0.17)	903(0.22)	801(0.11)	900	806
ring breathing (1)	756(0.84)	755(1.13)	747(0.81)	755	722
$1 + \rho_{\text{Me}}^s$	1856 ^c	1864 ^c	1765 ^c		

^a Relative intensities of bands are indicated inside parentheses. ^b From ref 25. ^c Bands are from ps-K-TR³ spectra shown in Figure 3.

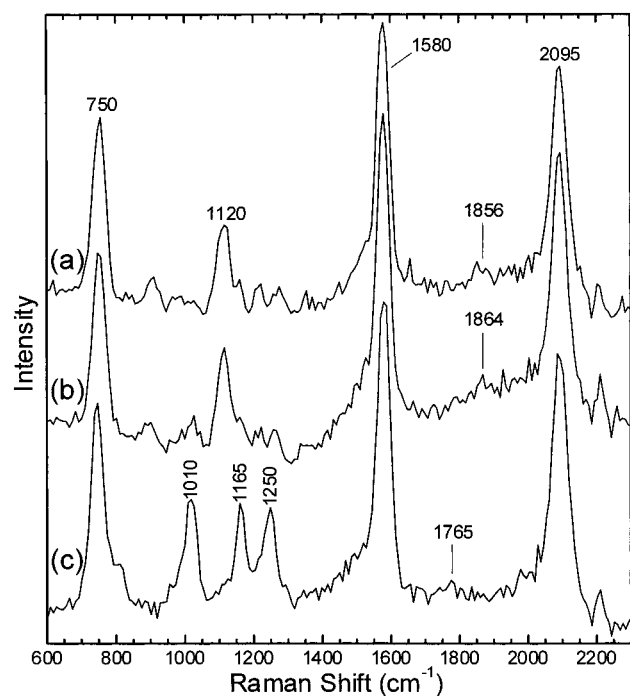


Figure 3. Picosecond Kerr gated time-resolved resonance Raman (ps-K-TR³) spectra of the A state of DMABN (a), DMABN-¹⁵N (b) and DMABN-*d*₆ (c) obtained by 267 nm pump, 330 nm probe in methanol at 50 ps delay time.

pump probe method. The close resemblance of all the spectral features to the corresponding ps-K-TR³ spectra demonstrates that these originate from the same state, the A state of DMABN. This observation is also supported by the position of the C≡N stretching frequency, which serves as a marker band to identify the state being probed.^{10,13,29} Complete subtraction of the ground state Raman signals is evident from the obvious difference between spectra in Figures 2 and 4. However, the ps-K-TR³ experiments were affected by the edge filter, which cut off bands below 700 cm⁻¹ and decreased the intensity of bands with frequency below 900 cm⁻¹.

The TR² data offer superior spectral resolution. For example, for DMABN and DMABN-¹⁵N, the broad strong asymmetric 1120 cm⁻¹ band observed using the picosecond apparatus is resolved into two bands at 1170 and 1116 cm⁻¹, and the weak features observed in the corresponding ps-K-TR³ spectra all appear more clearly. They are at 907, 984, 1221, and 1281 cm⁻¹ for DMABN and 903, 987, 1221, and 1261 cm⁻¹ for DMABN-

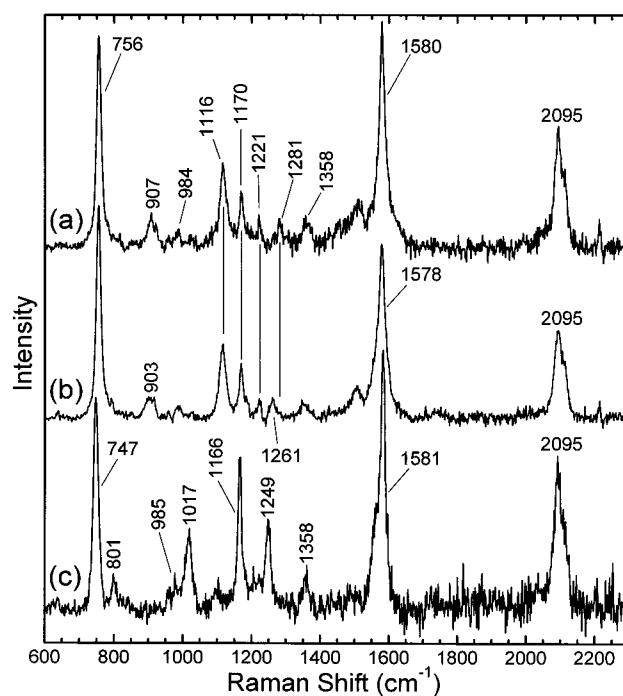


Figure 4. Transient resonance Raman (TR²) spectra of DMABN (a), DMABN-¹⁵N (b) and DMABN-*d*₆ (c) obtained by 330 nm excitation in methanol solvent.

¹⁵N. Two additional bands, at 1358 and 1502 cm⁻¹, are observed in the TR² spectra shown in Figure 4a,b. The shoulder on the high-frequency side of the intense 747 cm⁻¹ band in DMABN-*d*₆ (Figure 3c) is resolved into a band at 801 cm⁻¹ (Figure 4c). The 985 and 1358 cm⁻¹ bands are also observed in Figure 4c. Band frequencies and relative intensities computed from Lorentzian fitting of the spectra displayed in Figure 4 are listed in Table 2; their tentative assignment are also included and will be discussed below. Information from closely related compounds,²⁵ DMA-H⁺ and DMA-*d*₆-H⁺, are given in the table for comparison.

Transient Raman bands common to all the three compounds are observed at 756, 984, 1170, 1221, 1358, 1580, and 2095 cm⁻¹. IR measurements of the benzonitrile radical anion yielded bands at 760, 991, 1178, 1268, 1283, 1592, and 2093 cm⁻¹.³⁰ The similarity of these two groups of frequencies is striking and implies that the benzonitrile subgroup in the A state of DMABN resembles the benzonitrile radical anion and is thus consistent with a full charge transfer mechanism from the

dimethylamino to the benzonitrile group. These bands are insensitive to ^{15}N and methyl group deuteration, which further strengthens this observation. It is certain that, except for the 2095 cm^{-1} $\text{C}\equiv\text{N}$ stretching vibration, the other bands observed here belong to local phenyl ring modes. Assignments of these bands to totally symmetric modes (Table 2) are based on comparison with the ground state frequencies. The weak 1358 cm^{-1} band remains unassigned at present. It is clear that all the ring modes shift down on going from the ground state to the A state, in agreement with the A state structure and molecular orbitals suggested by the ICT mechanism¹ and theoretical calculations.^{7,8}

The bands at 1281 , 1116 , $907/1261$, 1115 , $903/1249$, 1017 , and 801 cm^{-1} in the spectra of DMABN, DMABN- ^{15}N , and DMABN- d_6 , are sensitive to isotopic substitution. Comparing Figure 4(a) with (b) and from Table 2, it is clear that two bands, at 1281 and 907 cm^{-1} , are sensitive to ^{15}N substitution. They show ~ 20 and $\sim 4\text{ cm}^{-1}$ downshift, respectively, on going from DMABN to DMABN- ^{15}N . This is strong evidence that these vibrations relate to the amino nitrogen atom. The extent and behavior of the observed isotopic shift is similar to the $\nu^s(\text{ph-N})$ and $\nu^s(\text{NC}_2)$ modes of the ground state. We note that Dreyer and Kummrow⁷ predict a 1286 cm^{-1} $\nu^s(\text{ph-N})$ frequency for the A state in the TICT model. We therefore attribute the $1281/1261\text{ cm}^{-1}$ (DMABN/DMABN- ^{15}N) band to the A state $\nu^s(\text{ph-N})$ mode and $907/903\text{ cm}^{-1}$ (DMABN/DMABN- ^{15}N) band to the A state $\nu^s(\text{NC}_2)$. Observation of these two modes in DMABN- d_6 is expected. From Figure 4c, it can be seen that the two bands are sensitive to deuteration of the methyl groups. Based on the isotopic shift observed in the ground state on going from DMABN to DMABN- d_6 , assignment of the DMABN- d_6 801 cm^{-1} band to the $\nu^s(\text{NC}_2)$ mode is straightforward. Attribution of the 1249 cm^{-1} (Figure 4c) band in DMABN- d_6 to the $\nu^s(\text{ph-N})$ vibration is supported by the Raman frequencies and isotopic shifts of the mode observed in DMA- H^+ and its methyl-deuterated counterpart DMA- $d_6\text{-H}^+$.²⁵ As recorded by Poizat et al.²⁵ frequencies of the $\nu^s(\text{ph-N})$ and $\nu^s(\text{NC}_2)$ modes were found to be 1245 and 900 cm^{-1} for DMA- H^+ , and 1205 and 806 cm^{-1} for DMA- $d_6\text{-H}^+$. The isotopic shifts are quite similar to our observations. It should be pointed out that, in methanol solvent, the $\sim 96\text{ cm}^{-1}$ $\nu^s(\text{ph-N})$ frequency downshift from the ground state (1377 cm^{-1} , Figure 1a) to the A state (1281 cm^{-1} , Figure 4a), as suggested by Dreyer and Kummrow,⁷ provides essential experimental evidence for the TICT model and rules out the PICT model. The downshift of the $\nu^s(\text{NC}_2)$ mode on going from the ground to the A state (944 to 907 cm^{-1}) is also consistent with the TICT model, as lengthening of the amino $\text{N}-\text{CH}_3$ bond is predicted by Dreyer and Kummrow.⁷

The remaining isotopically sensitive bands are 1116 cm^{-1} for DMABN and DMABN- ^{15}N , 1017 cm^{-1} for DMABN- d_6 . On close inspection of the spectra shown in Figure 3, one can see that weak bands at ~ 1860 and $\sim 1765\text{ cm}^{-1}$ appear in the spectra of DMABN/DMABN- ^{15}N and DMABN- d_6 , respectively. As no fundamental is expected in the $1700\text{--}2000\text{ cm}^{-1}$ range for para-substituted benzene derivatives,²⁷ the $\sim 1860\text{ cm}^{-1}$ band is assigned as a combination band of the 750 and 1120 cm^{-1} bands (Figure 3, a and b); the $\sim 1765\text{ cm}^{-1}$ band coincides with a combination of 750 and 1010 cm^{-1} (Figure 3c). We tentatively suggest that the 1017 cm^{-1} band in DMABN- d_6 is the counterpart of the 1116 cm^{-1} band in DMABN/DMABN- ^{15}N . The insensitivity of this mode to ^{15}N substitution and the $\sim 100\text{ cm}^{-1}$ frequency downshift upon deuteration of the methyl group implies the band is dominated by vibration of the amino group

methyl vibration. In the ground state, the ρ_{Me}^s mode shows similar isotopic shift behavior (Figure 2 and Table 1). We also note that the ρ_{Me}^s frequency was recorded to be 1132 and 1028 cm^{-1} for DMA- H^+ and DMA- $d_6\text{-H}^+$, respectively.²⁵ These are again comparable to bands we observed. The $1116/1017\text{ cm}^{-1}$ bands are therefore attributed to the ρ_{Me}^s vibration of the A state of DMABN compounds.

Discussion

The 330 nm excitation wavelength used for recording the ground state resonance Raman spectra (Figure 1) lies within the red tail of the lowest electronic absorption band. The ground state absorption spectra of the three DMABN compounds were all found to be similar. The two lowest singlet excited states are both dominated by phenyl ring $\pi\pi^*$ transitions, designated as L_a -type and L_b -type with transition moment parallel and perpendicular, respectively, to the molecular long axis, and constitute the absorption band.^{3,8,31} The oscillator strength of the L_b -type state is much less than the L_a -type state. In the gas phase or in nonpolar solvents, the L_b -type state is lower in energy.^{3,31,32} The absence of the methyl group rocking ρ_{Me}^s (1166 cm^{-1} band) in Figure 1 is consistent with the $\pi-\pi^*$ property of the transition.

When the Raman excitation wavelength is tuned to the maximum of the absorption band (300 nm) so as to probe the strong L_a -type transition, we find that the spectral pattern and relative intensity distribution changes significantly. This is manifested by extremely weak intensities of the two ring asymmetric modes, Wilson 8b (1546 cm^{-1}) and 14 (1324 cm^{-1}), and a remarkable decrease in the ratio of the 788 cm^{-1} band to other intense bands in the L_a -type transition. We therefore suggest that the 330 nm excitation spectra are dominated by the L_b -type transition and resonance enhancement of the three modes mentioned above occurs. This also implies that, even in a high-polarity solvent such as methanol, the L_b -type state is still of lower energy than the L_a -type state in the FC region. This is in agreement with the B fluorescence polarization measured in ethanol,³³ but casts doubt on results from several theoretical studies, which suggest that the L_a -type band lies below the L_b -type band in the FC region in polar solvents.^{32,34} It should be mentioned that the two asymmetric modes (Wilson 8b and 14), both of b_2 symmetry in the C_{2v} group, might be the vibrational modes coupling the LE ($1B_2$) and ICT ($1A_2$) potential energy surfaces.⁶

The geometry and electronic conformation of aromatic amino compounds has been studied extensively by both experimental²³⁻²⁵ and theoretical methods.^{16,26} It was shown that the $\nu^s(\text{ph-N})$ mode could be viewed as a good probe for evaluating the bonding configuration around the amino N atom and the electronic distribution of the aromatic amine compounds. The frequencies of typical single and double CN bonds are ~ 1200 and $\sim 1600\text{ cm}^{-1}$, respectively.²⁷ Depending on the extent of electronic coupling between the amino nitrogen lone pair electrons and the phenyl ring π system ($n\pi$ conjugation), the $\nu^s(\text{ph-N})$ frequency can change from being mainly single bond in character to having a significant degree of double bond character. For example, in the Raman study of DMA of Poizat et al.^{24,25} it was reported that the $\nu^s(\text{ph-N})$ frequency increases by $\sim 100\text{ cm}^{-1}$ on going from the protonated (1245 cm^{-1}) DMA, DMA- H^+ , to neutral (1348 cm^{-1}) form, and by a further $\sim 20\text{ cm}^{-1}$ on forming the radical cation (1366 cm^{-1}). The geometries of the neutral and radical cation of DMA are near planar (27° wagging angle) and planar, respectively, implying extensive $n\pi$ conjugation interaction and thus the sp^2 character of the amino

N atom.^{16,24} For DMA-H⁺, involvement of the lone pair in a N–H bond leads to substantial electronic decoupling from the ring π system, therefore changing the amino group from planar sp² to a pure pyramidal sp³ hybridization conformation,²⁵ as for saturated pyramidal alkyl substituted amines. This has been verified by the similarity of the ring–N bond length of the protonated aromatic amino compounds to that of typical single C–N bonds of α -amino acids, as determined by X-ray diffraction measurements.³⁵

The structure of crystalline DMABN has been determined from X-ray diffraction data to be slightly nonplanar with $\sim 11^\circ$ wagging angle.³⁶ Its amino conformation is therefore similar to that in DMA, TMPD (15° wagging angle) and other aromatic dimethylamino compounds.^{23,24,26} Similarity of frequencies and isotopic shift behavior of modes related to the amino group, such as the $\nu^s(\text{ph-N})$, $\nu^s(\text{NC}_2)$, and ρ_{Me}^s , between ground state of DMABN recorded here and those compounds confirm this. The higher $\nu^s(\text{ph-N})$ frequency in DMABN (1370 cm^{-1}) than DMA (1348 cm^{-1}) shows that a stronger $n\pi$ interaction is induced by the *p*-amino cyano group. Vibrational mixing of the $\nu^s(\text{ph-N})$ with the phenyl ring C=C 19a and methyl groups is observed generally in near-planar or planar aromatic amino compounds^{23–25} and has been verified by theoretical calculation.¹⁶ This is manifested in the ground state of DMABN as a 5 cm^{-1} downshift for Wilson 19a upon ¹⁵N substitution and 7 cm^{-1} downshift upon methyl deuteration.

For the A state of DMABN, the $\sim 96\text{ cm}^{-1}$ downshift of this mode compared with the ground state implies a substantial decrease in the $n\pi$ interaction and electronic isolation of the amino from the benzonitrile subgroups, and is similar to the $\sim 100\text{ cm}^{-1}$ decrease in $\nu^s(\text{ph-N})$ frequency on going from DMA to DMA-H⁺.²⁵ This is in good agreement with the minimum overlap principle of the TICT model¹ but opposite to the strong electronic coupling proposed by the PICT model.⁴ As stressed by Rettig et al.³¹ and supported by some theoretical studies,^{6,32} a 90° twisting and “antipyramidalization” (sp² hybridization) conformation of the amino group is thought to be important in the TICT model. However, as illustrated above, the resemblance of the amino-related modes ($\nu(\text{ph-N})$, $\nu^s(\text{NC}_2)$, and ρ_{Me}^s) of A state DMABN and DMA-H⁺, which has pyramidal sp³ hybridization, casts doubt on this. A decrease of $\nu^s(\text{NC}_2)$ frequency ($\sim 37\text{ cm}^{-1}$) on going from the ground to the A state also indicates an sp³ pyramidal character of the A state amino group. Theoretical studies^{6,8,37} show that a wagging motion of the DMABN amino group cannot by itself lead to a stable highly polar excited state. Substantial twisting combined with some wagging of the amino group might be a more realistic conformation for the A state, as has been suggested by the CASSCF study of DMABN of Serrano-Andres et al.³⁸ In addition, oscillator strength calculation indicated that electronic dipole-induced transition from the A state with 90° twisting geometry to the ground state is forbidden by symmetry, therefore, a structure with the twisting angle deviating from 90° has been proposed for the A state to interpret the strong red fluorescence observed in experiments.³⁹ Such a partial twisting structure was also suggested by ab initio studies carried out by Parusel et al. (60° twisting angle)⁸ and Sobolewski et al. (45° twisting angle).⁹ It was shown by previous calculations that, with the wagging angle constrained to 0° , the shape of the ICT state potential surface along the twisting angle is strongly dependent on the level of theory used such that the lowest energy occurs at planar,³⁷ perpendicular⁷ or intermediate twisting angle.^{8,9} A full optimization of the A state structure considering both the twisting and wagging motion and also including

possible solvation effects is still lacking; however, it is hoped that the data presented here can stimulate this much needed work.

It is interesting to observe the influence that deuteration of the aminomethyl groups has on the Raman spectra. The $\nu^s(\text{ph-N})$ frequency of the ground state is little affected by methyl deuteration. However, this mode in the A state is sensitive and gives a $\sim 32\text{ cm}^{-1}$ downshift upon deuteration possibly indicating an increase in the coupling between the $\nu^s(\text{ph-N})$ mode and the modes associated with the methyl group. Such an increase in the coupling of vibrational modes is observed in nonaromatic amino compounds, (CH₃)₂N–X. For example, calculations⁴⁰ of the potential energy distribution and frequency of these compounds indicate that the N–X stretching mode is strongly coupled with a methyl rocking vibration. This supports the electronic decoupling of the amino group from the aromatic ring as envisaged by the twisted A state.

Among the three TRIR bands recorded by Okamoto¹² two bands, at 1216 and 1273 cm^{-1} , are observed in our 330 nm transient Raman spectrum, that is corresponding to the 1221 and 1281 cm^{-1} bands in Figure 4a. As discussed above, these are assigned to the $\nu^s(\text{ph-CN})$ and $\nu^s(\text{ph-N})$ mode, respectively, and this is consistent with the results of Okamoto.¹² The strong TRIR band at 961 cm^{-1} is within experimental error of the 957 cm^{-1} band presented in our previous published ps-K-TR³ spectra obtained with 400 nm excitation wavelength.¹⁴ It was attributed to a phenyl ring mode because of its insensitivity to methyl group deuteration.

Although the spectral profiles of DMABN and DMABN-¹⁵N are very similar (see Figures 3 and 4), there are significant differences from DMABN-*d*₆ in the 900–1300 cm^{-1} region. As mentioned in our previous paper, this indicates a large difference in potential energy distribution in either the A or the upper electronic state, or both, for DMABN/DMABN-¹⁵N and DMABN-*d*₆. Such a methyl group deuteration sensitivity has been reported for several aromatic amino compounds.^{16,24}

Conclusion

The ps-K-TR³ spectra of DMABN, DMABN-¹⁵N, and DMABN-*d*₆ have been recorded at 330 nm probe wavelength. TR² spectra with improved spectral resolution have also been obtained using 330 nm single-color pump–probe (TR²) excitation. From these results it has been possible to identify the crucial $\nu^s(\text{ph-N})$ mode of the DMABN A state intermediate at 1281 cm^{-1} . Nonresonant and 330 nm resonance Raman spectra of the ground state of the three compounds have also aided vibrational assignments of the three amino group related modes, the $\nu^s(\text{ph-N})$, $\nu^s(\text{NC}_2)$, and ρ_{Me}^s . The $\sim 96\text{ cm}^{-1}$ downshift of the $\nu^s(\text{ph-N})$ mode on going from the ground to A state provides unequivocal evidence of electronic decoupling of the amino from the benzonitrile group in the A state. The resemblance of the C \equiv N stretching and ring local mode frequencies of the A state to those found in the benzonitrile radical anion is consistent with the full ICT charge-transfer mechanism and indicates localization of the charge following the ICT reaction. The work presents substantial evidence in support of the TICT model for the ICT structure of DMABN. However, the spectroscopic similarities with protonated dimethylaniline (DMA-H⁺) indicate that the A state of DMABN has some pyramidal character.

Acknowledgment. We are grateful to the EPSRC for financial support through grants GR/K20989 and GR/L84001. W.M.K. gratefully acknowledges financial support from the

Croucher Foundation, Hong Kong. S.U. thanks Imperial College for providing a visiting fellowship and financial support to collaborate in this work. We thank Dr. Ian Clark for his assistance in the TR² experiments. This work was carried out within the Central Laser Facility, CLRC Rutherford Appleton Laboratory.

References and Notes

- (1) Lippert, E.; Rettig, W.; Bonacic-Koutecky, V.; Heisel, F.; Miehe, J. A. *Adv. Chem. Phys.* **1987**, *68*, 1.
- (2) Rotkiewicz, K.; Grelmann, K. H.; Grabowski, Z. R. *Chem. Phys. Lett.* **1973**, *19*, 315.
- (3) Schuddeboom, W.; Jonker, S. A.; Warman, J. M.; Leinhos, U.; Kuhnle, W.; Zachariasse, K. A. *J. Phys. Chem.* **1992**, *96*, 10809.
- (4) Zachariasse, K. A.; Grobys, M.; Von der Haar, T.; Hebecker, A.; Ilchev, Y. V.; Jiang, Y.-B.; Morawski, O.; Kuhnle, W. *J. Photochem. Photobiol. A: Chem.* **1996**, *102*, 59.
- (5) Sobolewski, A. L.; Domcke, W. *Chem. Phys. Lett.* **1996**, *259*, 119.
- (6) Sudholt, W.; Sobolewski, A. L.; Domcke, W. *Chem. Phys.* **1999**, *240*, 9.
- (7) Dreyer, J.; Kummrow, A. *J. Am. Chem. Soc.* **2000**, *122*, 2577.
- (8) Parusel, A. B. J.; Kohler, G.; Grimme, S. *J. Phys. Chem. A* **1998**, *102*, 6297.
- (9) Sobolewski, A. L.; Sudholt, W.; Domcke, W. *J. Phys. Chem. A* **1998**, *102*, 2716.
- (10) Hashimoto, M.; Hamaguchi, H. *J. Phys. Chem.* **1995**, *99*, 7875.
- (11) Chudoba, C.; Kummrow, A.; Dreyer, J.; Stenger, J.; Nibbering, E. T. J.; Elsaesser, T.; Zachariasse, K. A. *Chem. Phys. Lett.* **1999**, *309*, 357.
- (12) Okamoto, H. *J. Phys. Chem. A* **2000**, *104*, 4182.
- (13) Kwok, W. M.; Ma, C.; Phillips, D.; Matousek, P.; Parker, A. W.; Towrie, M. *J. Phys. Chem. A* **2000**, *104*, 4189.
- (14) Kwok, W. M.; Ma, C.; Matousek, P.; Parker, A. W.; Phillips, D.; Toner, W. T.; Towrie, M. *Chem. Phys. Lett.* **2000**, *322*, 395.
- (15) Gates, P. N.; Steele, D.; Pearce, R. A. R.; Radcliffe, K. J. *Chem. Soc., Perkin Trans. 2* **1972**, 1607.
- (16) Brouwer, A. M.; Wilbrandt, R. *J. Phys. Chem.* **1996**, *100*, 9678.
- (17) Schneider, S.; Freunshcht, P.; Brehm, G. *J. Raman Spectrosc.* **1997**, *28*, 305.
- (18) Matousek, P.; Parker, A. W.; Taday, P. F.; Toner, W. T.; Towrie, M. *Opt. Commun.* **1996**, *127*, 307.
- (19) Towrie, M.; Parker, A. W.; Shaikh, W.; Matousek, P. *Meas. Sci. Technol.* **1998**, *9*, 816.
- (20) Matousek, P.; Towrie, M.; Stanley, A.; Parker, A. W. *Appl. Spectrosc.* **1999**, *53*, 1485.
- (21) Mitchell, R. H.; Chen, Y.; Zhang, J. *Org. Prep. Proced. Int.* **1997**, *29*, 715.
- (22) Friedman, L.; Shechter, H. *J. Org. Chem.* **1961**, *26*, 2522.
- (23) Tripathi, G. N. R.; Schuler, R. H. *Chem. Phys. Lett.* **1984**, *110*, 542.
- (24) Poizat, O.; Guichard, V. *J. Chem. Phys.* **1989**, *90*, 4697.
- (25) Guichard, V.; Bourkba, A.; Lautie, M.-F.; Poizat, O. *Spectrochim. Acta* **1989**, *45A*, 187.
- (26) Kushto, G. P.; Jagodzinski, P. W. *Spectrochim. Acta, Part A* **1998**, *54*, 799.
- (27) Varsanyi, G. In *Assignments for vibrational spectra of seven hundred benzene derivatives*; Lang, L., Ed.; Adam Hilger: London, 1974; Vol. 1.
- (28) Okada, T.; Uesugi, M.; Kohler, G.; Rechthaler, K.; Rotkiewicz, K.; Rettig, W.; Grabner, G. *Chem. Phys.* **1999**, *241*, 327.
- (29) Forster, M.; Hester, R. E. *J. Chem. Soc., Faraday Trans. 2* **1981**, *77*, 1535.
- (30) Juchnovski, I.; Tsvetanov, C.; Panayotov, I. *Monatsh. Chem.* **1969**, *100*, 1980.
- (31) Rettig, W.; Zietz, B. *Chem. Phys. Lett.* **2000**, *317*, 187.
- (32) Gedeck, P.; Schneider, S. *J. Photochem. Photobiol. A: Chem.* **1997**, *105*, 165.
- (33) Rettig, W.; Wermuth, G.; Lippert, E. *Ber. Bunsen-Ges. Phys. Chem.* **1979**, *83*, 692.
- (34) Cammi, P.; Mennucci, B.; Tomasi, J. *J. Phys. Chem. A* **2000**, *104*, 5631.
- (35) Chandrasekaran, R. *Acta Crystallogr.* **1969**, *B25*, 369.
- (36) Heine, A.; Irmer, R. H.; Stalke, D.; Kuhnle, W.; Zachariasse, K. A. *Acta Crystallogr.* **1994**, *B50*, 363.
- (37) Gorse, A.-D.; Pesquer, M. *J. Phys. Chem.* **1995**, *99*, 4039.
- (38) Serrano-Andres, L.; Merchán, M.; Roos, B. O.; Lindh, R. *J. Am. Chem. Soc.* **1995**, *117*, 3189.
- (39) Calzaferri, G.; Rytz, R. *J. Phys. Chem.* **1995**, *99*, 12141.
- (40) Finch, A.; Hyams, I. J.; Steele, D. *J. Mol. Spectrosc.* **1965**, *16*, 103.